CONF-921147--1

# EROSION OF COMPOSITE CERAMICS*

J. L. Routbort

*Materials Science Division*
*Argonne National Laboratory*
*Argonne, IL 60439–4838*

ANL/CP--75338

DE93 004254

August 1992





**INVITED KEYNOTE** manuscript to be presented at the 8th International Symposium on Ceramics (8th SIMCER), Rimini, Italy, 10-12 November 1992. Proceedings to be published in a regular issue of Acta Ceramico.

*This work supported by the U.S. Department of Energy, Basic Energy Sciences–Materials Science, under Contract W-31-109-ENG-38.

# Erosion of Composite Ceramics

J. L.. Routbort

Materials Science Division, Argonne National Laboratory, Argonne, Illinois 60439–4838 (USA)

*ABSTRACT*

The theoretical basis to describe solid-particle erosion of monolithic ceramics is well developed. In many cases, the models can account for the impact velocity, impact angle and erodent-size dependencies of the steady-state erosion rate. In addition, the models account for effects of materials parameters such as fracture toughness and hardness. Steady-state erosion measurements on a wide variety of composite ceramics, including SiC whisker-reinforced $Al_2O_3$, $Si_3N_4$ containing $Si_3N_4$ or SiC whiskers, $Y_2O_3$-stabilized $ZrO_2$ reinforced with SiC whiskers, and duplex-microstructure $Si_3N_4$ have been reported. The theories developed for monolithic ceramics are, however, less successful in describing the results for composites.

## *I. INTRODUCTION*

The resistance of a brittle material to solid-particle erosive wear depends on the properties of the impacting erodent and on some materials properties of the target. Erosion resistance of a given ceramic can be altered by tailoring the microstructure, which changes the erosion-sensitive materials properties. A recent review covers most of the aspects of erosion of brittle solids [1]. Material loss upon impact by an angular erodent occurs by formation and propagation of lateral cracks to the surface under the driving forces imposed by the particle impact events [2]. Both dynamic [2] and quasi-static [3] models of erosion predict that the steady-state erosion rate, $\Delta W$ (amount of target removed for amount of abrasive hitting the target in units of g/g), is proportional to a power law of the form,

$$\Delta W \propto V^n D^{2/3} \rho^p (K_{IC})^{-4/3} H^q ,$$

where V, D, and $\rho$ are the impacting particle velocity, mean diameter, and density, respectively. The materials parameters are the fracture toughness, $K_{IC}$, and the hardness, H. It should be mentioned that the static $K_{IC}$ and H are used, because of lack of information on the dynamic values.

The constant of proportionality differs for different assumptions, and may include other factors, depending on the contact model used. In general, the velocity exponent, n, varies between about 2.0 and 3.2, depending on erodent shape and the contact conditions. The density exponent is about 1.2. The dependence on H is weak, with the exponent varying between -0.24 and 0.11. Therefore, it is expected that, under a given set of erosive conditions, $K_{IC}$ will have the largest effect on erosion resistance.

Strength and fracture toughness of monolithic ceramics can be significantly enhanced by addition of ceramic whiskers. The improvement in toughness is related to fiber sliding, crack deflection, crack bowing, and/or microcrack formation [4]. Examples of ceramics in which enhanced toughening from whisker additions has been observed include: $Al_2O_3$ [5], $Si_3N_4$ [6], toughened $ZrO_2$ [7], $MoSi_2$ [8], and magnesia-alumina spinels [9]. Indeed, Becher and Wei [5] have shown that $K_{IC}$ of $Al_2O_3$ can be doubled by adding 20 vol.% SiC whiskers. Various types of whiskers are available, e.g., SiC, $Si_3N_4$ and $Al_2O_3$, with the first being the most common. Toughening can also be accomplished by microstructure manipulation: an example being an "*in-situ*" reinforced $Si_3N_4$. The microstructure of this high-toughness material is characterized by a bimodal grain distribution. The long-crack-length-limit fracture toughness is about 50% higher than that of an equivalent fine-grained $Si_3N_4$ [10]. The increased toughness should result in an enhanced erosion resistance and, therefore, possible applications for these hard, new materials are ones in which the materials are subjected to erosion by solid particles, e.g., pump vanes, fuel regulators for jet engines, cutting tools, etc.

Erosion has been measured in the $Al_2O_3$-SiC(w) system (where (w) denotes whisker) by Sykes et al. [11] and Wada et al. [12], the $Si_3N_4$-SiC(w) system [13,14], the $Si_3N_4$-$Si_3N_4$(w) system, and on an $Y_2O_3$-stabilized-$ZrO_2$ (TZ3Y)-$Al_2O_3$(w) composite [15]. Recently [10], erosion and R-curve results have been reported on *in-situ* reinforced and an equivalent fine-grained $Si_3N_4$. The effect of erosion damage on the strength in an *in-situ* reinforced $Si_3N_4$ has also been reported [16].

This paper will review some of the erosion results for various modern structural ceramics. Trends in the behavior of the steady-state erosion rates with the principal variables (V and $K_{IC}$) will be compared to theoretical predictions. It is interesting and important to investigate erosion behavior of these materials and

to develop the capability to predict the materials loss, given all of the properties of the erodent and the target material.

## *II. EXPERIMENTAL PROCEDURES*

Details of the sample preparation and characterization are given in the original references. Briefly, the $Al_2O_3$ composites used for these tests were obtained from Advanced Composite Materials, Greer, South Carolina. Compositions were supplied with 0, 5, 15, and 25 wt.% SiC whiskers. Whiskers were approximately 1 μm in diameter with an average length of 30 μm. Fracture toughness varied from 3.8 to 6.8 $MPam^{1/2}$ as the whisker concentration was increased to 25 wt.% [11].

The $Si_3N_4$ composites containing $Si_3N_4$(w) or SiC(w) were fabricated from powders and whiskers by hot-pressing, with MgO as a sintering aid. The $K_{IC}$ varied from 6.4 to 7.5 $MPam^{1/2}$ as the 0.6 μm diameter $Si_3N_4$ whisker concentration increased from 0 to 15 vol.% [17], whereas the toughness of the SiC(w) composite increased from 4 to 7 $MPam^{1/2}$ as the whisker concentration increased to 20 wt.% [6].

Zirconia composites were prepared by hot-pressing mixtures of 3 mol.% $Y_2O_3$ tetragonal-stabilized zirconia (TZ3Y) with 4-7 μm diameter $Al_2O_3$ whiskers. The $K_{IC}$ values were 8.6, 7.5 and 10 $MPam^{1/2}$ for the 0, 15 and 25 vol.% compositions, respectively [15].

The duplex microstructure $Si_3N_4$ was produced by Allied-Signal, Morristown, New Jersey. This *in-situ* reinforced material has a pronounced R-curve behavior with a long-crack length toughness of 8.3 $MPam^{1/2}$, compared to an equivalent fine-grained $Si_3N_4$ having a toughness of 5.6 $MPam^{1/2}$ [10].

Measurements were carried out in a slinger-type apparatus [18]. Velocities of impact were varied between 40 and 140 m/s and angular SiC or $Al_2O_3$ abrasives

having mean diameters from 40-1000 μm were used. The effect of the ratio of the erodent hardness to that of the target has been discussed [14, 19, 20]. The angle of incidence was usually varied from 15 to 90°, but this paper will concentrate on results obtained at normal incidence.

## *III. RESULTS AND DISCUSSION*

Typical erosion data are presented in Fig. 1, which was obtained for two ceramics and their whisker composites impacted by 42 μm diameter SiC abrasives at normal incidence and 100 m/s. After an initial transient, the slope of the weight loss versus dose impacting the sample becomes constant and is, by definition, equal to the steady-state erosion rate. Discussion in this paper will be confined to the steady state. Steady-state erosion rates obtained in this manner, using 143 μm diameter SiC abrasives impacting an $Al_2O_3$-SiC (w) composite, are presented in Fig. 2. A general observation for all composite ceramics measured is that the velocity dependence of $\Delta W$ is indeed exponential. The velocity exponents, n, at normal incidence are tabulated in Table 1 for a variety of composites using two types of erodents.

The striking feature of Table 1 is that there is a wide discrepancy between n-values obtained for the softer $Al_2O_3$ than for the harder SiC abrasive. The explanation lies in the fact that the composite can be harder than the erodent [14, 19, 20] and considerable energy is expended in fracture and blunting of the impacting particle, energy which is unavailable for nucleation and propagation of lateral cracks which control erosion. Even the hard SiC abrasives fracture, as illustrated in Fig. 3 which shows scanning electron microscopy (SEM) micrographs of SiC abrasives before and after impacting a $Si_3N_4$ target. It is seen that the mean of the size distribution of the spent erodent is smaller than that of the initial distribution. Larger particles fragment more than smaller particles [15],

but recent results [10] using a $Si_3N_4$ target indicate that fragmentation of SiC or $Al_2O_3$ erodents is identical. For the harder erodents, the n values are, for the most part, in accord with the theoretical predictions and comparable to those measured for monolithic ceramics [1].

Softer particles remove material less efficiently than do harder particles. This is illustrated in Fig. 4, which shows that, depending on the erodent, $\Delta W$ can differ by a least an order of magnitude [20]. The erosion rate of both unreinforced and reinforced ceramics depend on the erodent. The results typified by Fig. 4 are confirmed by SEM micrographs of the surfaces eroded by single particles or into steady state. The micrographs display differences that depended on the type of erodent. Surfaces eroded by softer erodents indicate that particle crushing occurs because some of the crushed erodent adhered to the impact site. The surface of the composite eroded by the harder material has sharper features and contains more cracks. There was no evidence that the materials removal mechanism changed, only the rate. Scattergood and coworkers [19, 21] concluded from a series of experiments with different $Al_2O_3$ targets that for the softer erodents more damage accumulation is necessary to build up requisite stresses to produce lateral cracks.

The simple theories fail to predict, in all cases, the dependence of $\Delta W$ on $K_{IC}$, as shown in Fig. 5. It can be seen that the predicted slope of -4/3, as shown by the solid line, fits the experimental results for the $Al_2O_3$-SiC(w) composite, but not for the other composites. For each of these other composites, increases in erosion resistance have been offset by changes which are detrimental to erosion. For example, the increase in toughness in the $Si_3N_4$-SiC(w) system is believed to be due to microcracking due to presence of a grain boundary glass phase [6] which, while increasing $K_{IC}$, would help propagate the lateral cracks responsible for

erosion [17]. Therefore, not all toughening processes decrease $\Delta W$ and the models must be applied with caution.

R-curve behavior has been invoked to explain the failure of $\Delta W$ to be proportional to $(K_{IC})^{-4/3}$ for a series of partially stabilized zirconias (PSZ) [22]. Srinivasan and Scattergood point out that the correct toughness is that value relevant for the size scale of the erosion-impact events, $K^{op}$. The latter can be significantly less than the maximum toughness. In fact, they found a good correlation between $\Delta W$ and $K^{op}$, which was determined from the intersection of the stress intensity factor and the crack driving force. Recent measurements on a fine-grained and an "*in-situ*" reinforced $Si_3N_4$ show that $\Delta W$ is nearly independent of the material, despite the differences in the R-curve behavior [10]. This result has been interpreted as being due to the fact that the toughness is determined by crack initiation and is consistent with the $K^{op}$ concept. Nevertheless, it should be pointed out that in these tough, hard composites the operative toughness is that determined for short crack lengths, and it is precisely that region of the R-curve which is very difficult to measure.

Another factor to consider in the design of structural ceramics for use in an erosive environment is that materials suffer strength degradation as a result of crack formation during impact [16]. A result for an "*in-situ*" reinforced $Si_3N_4$ produced by Allied-Signal, Inc., is shown in Fig. 6. In this experiment, the sample was eroded into steady state at three velocities using 143 μm mean diameter $Al_2O_3$ erodents. Biaxial flexure strength in a series of ten samples that were eroded simultaneously under the same conditions was measured. The strength decreases by 20% for a velocity increase of about 2.8.

## *IV. CONCLUSIONS*

Designing or choosing composite or structural ceramics for applications in an erosive environment must be done with care. The models of erosion developed for monolithic ceramics may not be fully valid, especially if the hardness of the target exceeds that of the erodent. In this case, particle fragmentation becomes important. Additionally, while many mechanisms can be used to toughen a composite, some of these mechanisms may not lead to an increased erosion resistance. R-curve behavior and an operative toughness are important considerations. Erosion damage will always decrease fracture strength.

## *ACKNOWLEDGMENTS*

The author is grateful to a large number of students and colleagues who have contributed to this work over the last decade. In particular, he is grateful to Amy Thompson for providing the strength data and to Dr. K. C. Goretta who critically read the manuscript. This work was supported by the U.S. Department of Energy, Basic Energy Sciences–Materials Science, under Contract W-31-109-ENG-38.

*REFERENCES*

[1] J.L. Routbort and R.O. Scattergood, in Erosion of Ceramic Materials, ed. by J. E. Ritter, Trans Tech Publication, Switzerland (1992), pp. 23-51.

[2] A.G. Evans, M.E. Gulden and M.E. Rosenblatt, Proc. Roy. Soc. London, Ser. A361, 343-365 (1979).

[3] S.M. Wiederhorn and B.R. Lawn, J. Am. Ceram. Soc. 62, 66-70 (1979).

[4] R.W. Rice, Ceram. Eng. Sci. Proc. 2, 661-701 (1981).

[5] P.F. Becher and G.C. Wei, J. Am. Ceram. Soc. 67, C267-269 (1984).

[6] J.P. Singh, K.C. Goretta, D.S. Kupperman and J.L. Routbort, Adv. Ceram. Mater. 3, 357-360 (1988).

[7] N. Claussen and G. Petzow, Tailoring of Multiphase and Composite Ceramics, Plenum Publishing Corp., New York (1986), pp. 649-662.

[8] F.D. Gac and J.J. Petrovic, J. Am. Ceram. Soc. 68, C200-201 (1985).

[9] P.C. Panda and E.R. Seydel, Amer. Ceram. Soc. Bull. 65, 338-341 (1986).

[10] M. Marrero, J.L. Routbort, P. Whalen, C.-W. Li and K.R. Karasek, Wear, in press.

[11] M.T. Sykes, R.O. Scattergood and J.L. Routbort, Composites 18, 153-163 (1987).

[12] S. Wada, N. Watanabe and T. Tam, J. Ceram. Soc. Jpn. Inter. Ed. 96, 113-119 (1988).

[13] C. T. Morrison, J.L. Routbort and R.O. Scattergood, Mater. Res. Soc. Symp.Proc. 78, 207-214 (1987).

[14] S. Wada, N. Watanabe, T. Tani and O. Kamigaito, in Structural Ceramics, Fracture Mechanics, vol. 5, eds. M. Doyama, S. Somiya and R. Chang, Mater. Res. Soc., Pittsburg, PA (1989), pp. 481-490.

[15] J.L. Routbort, D.A. Helberg and K.C. Goretta, J. Hard Mater. 1, 123-135 (1990).

[16] J.E. Ritter, S.R. Choi, K. Jankus, P.J. Whalen, and R.G. Rateick, J. Mater. Sci. 26, 5543-5546 (1991).

[17] J.L. Routbort, K.C. Goretta, C.-Y. Chu, and J.P. Singh, in Tribology of Composite Materials, eds. P.K. Rohatgi, P.J. Blau and C.S. Yust, ASM, Materials Park, OH (1990) pp. 355-360.

[18] T.H. Kosel, R.O. Scattergood and A.P.L. Turner, Wear of Materials, ASME, NY, (1979), pp. 192-204.

[19] S. Srinivasan and R.O. Scattergood, Wear 128, 139-52 (1988).

[20] J.L. Routbort, C.-Y.Chu, J.M. Roberts, J.P. Singh, W. Wu and K.C. Goretta, Proceedings Corrosion-Erosion-Wear of Materials at Elevated Temperatures, ed. by A.V. Levy, National Assoc. of Corrosion Engrs., Houston, TX (1991), pp. 31-1-31-9.

[21] L.M. Murugesh and R.O. Scattergood, J. Mater. Sci. 26, 5456-5466 (1991).

[22] S. Srinivasan and R.O. Scattergood, Adv. Ceram. Mater. 3, 345-352 (1988).

Table I. Values of the velocity exponent, n, in $\Delta W \propto V^n$, measured for various structural ceramics at normal incidence using SiC and $Al_2O_3$ erodents.

| Material | Velocity [m/s] | n 143 μm-SiC | n 143 μm-$Al_2O_3$ | References |
|---|---|---|---|---|
| $Al_2O_3$ | 40-100 | 2.3 | 2.3 | 11,15 |
| $Al_2O_3$-5% SiC(w) | 40-100 | 2.5 | 1.7 | 11,15 |
| $Al_2O_3$-15% SiC(w) | 40-100 | 2.1 | 0.7 | 11,15 |
| $Al_2O_3$-25% SiC(w) | 40-100 | 2.0 | 1.1 | 11,15 |
| $Si_3N_4$ | 40-100 | 2.7 | | 15 |
| $Si_3N_4$-5% $Si_3N_4$(w) | 40-100 | 2.6 | | 15 |
| $Si_3N_4$-15% $Si_3N_4$(w) | 40-100 | 2.8 | | 15 |
| TZ3Y | 40-100 | 2.8 | | 15 |
| TZ3Y-15% $Al_2O_3$(w) | 40-100 | 2.8 | | 15 |
| TZ3Y-25% $Al_2O_3$(w) | 40-100 | 2.7 | | 15 |
| $Si_3N_4$ | 80-140 | | 2.6* | 13 |
| $Si_3N_4$-10v % $Si_3N_4$(w) | 80-140 | | 2.4* | 13 |
| $Si_3N_4$-20 v% $Si_3N_4$(w) | 80-140 | | 2.2* | 13 |
| $Si_3N_4$-fine grain | 50-100 | 2.4 | | 10 |
| $Si_3N_4$-*in situ* | 50-100 | 2.1 | | 10 |

*measured using 63 μm diameter erodents

*Figure Captions*

Fig. 1. Weight loss versus erodent dose for 42 μm diameter SiC particles impacting at normal incidence at 100 m/s for $Al_2O_3$ (open squares), $Al_2O_3$-25 wt.% SiC(w) (open triangles), $Si_3N_4$ (filled squares), and $Si_3N_4$-15 vol.% $Si_3N_4$(w) (filled triangles).

Fig. 2. Steady-state erosion rates at normal incidence for a series of $Al_2O_3$-SiC(w) composites using 143 μm diameter SiC erodents. The weight percent of whiskers of each composite is: open circles–0%, open squares–5%, open triangles–15%, and solid circles–25%.

Fig. 3. Scanning electron microscopy of 143 μm diameter SiC erodent: 3A–as received and 3B–after impacting a $Si_3N_4$ specimen at 100 m/s at normal incidence. The marker is 100 μm.

Fig. 4. Steady-state erosion rate measured at normal incidence for an impacting velocity of 100 m/s using 143 μm diameter erodents of SiC (circles), $Al_2O_3$ (squares) and a 75% $Al_2O_3$ - 25% $ZrO_2$ abrasive (triangles).

Fig. 5. Steady-state erosion rate versus $1/K_{IC}$ for four whisker-reinforced composites measured using 143 μm diameter SiC abrasives. Symbols are $Si_3N_4$ (squares), $Al_2O_3$-SiC(w) (open circles), $Si_3N_4$-SiC(w) (filled circles) and $Y_2O_3$-stabilized $ZrO_2$-$Al_2O_3$(w) (triangles).

Fig. 6. Fracture stress of an "*in-situ*" reinforced $Si_3N_4$ versus 143 μm mean diameter $Al_2O_3$ particle impact velocity under steady-state erosion conditions.

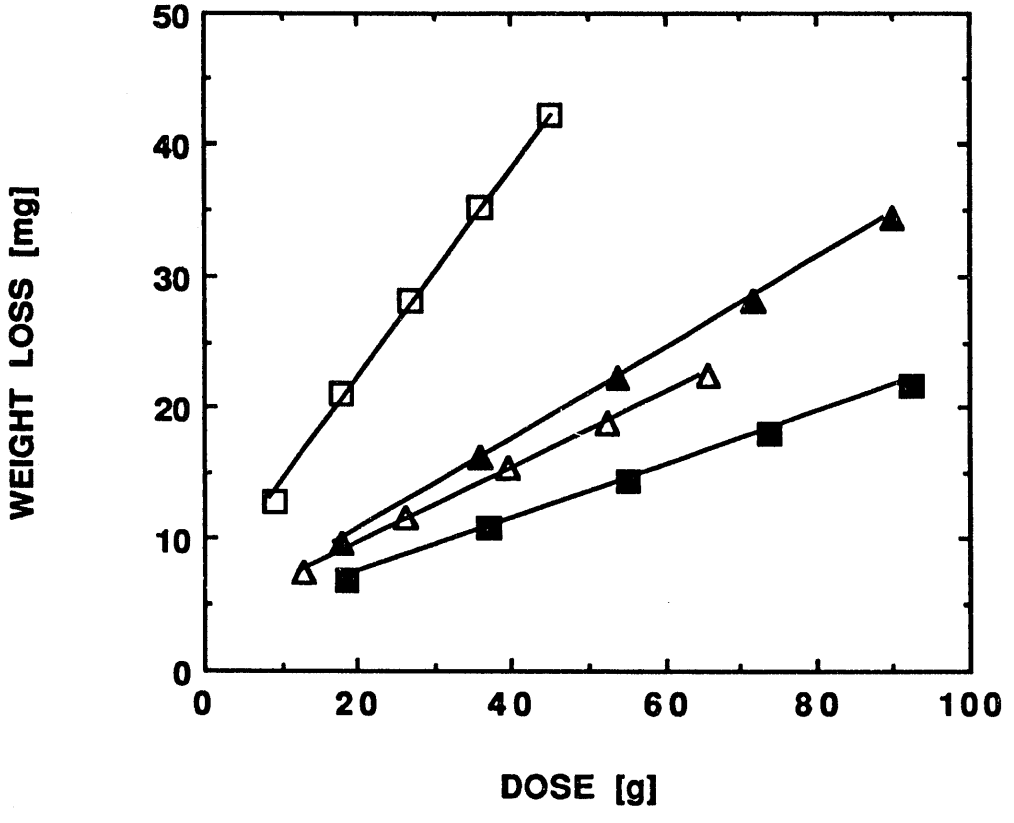


Figure 1. Weight loss versus erodent dose for 42 μm diameter SiC particles impacting at normal incidence at 100 m/s for $Al_2O_3$ (open squares), $Al_2O_3$-25 wt.% SiC(w) (open triangles), $Si_3N_4$ (filled squares), and $Si_3N_4$-15 vol.% $Si_3N_4$(w) (filled triangles).

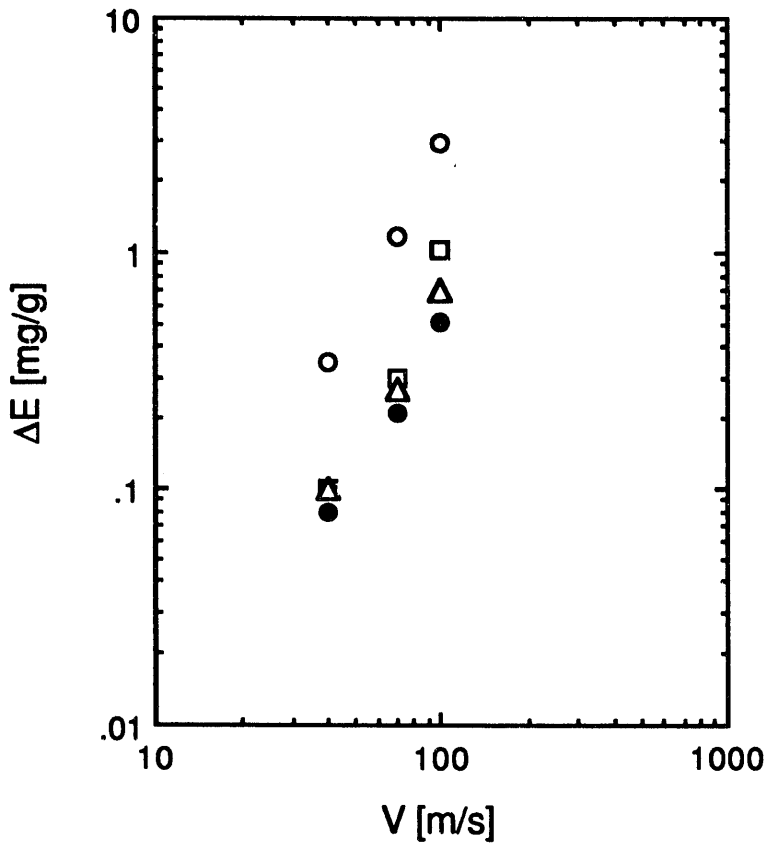


Figure 2. Steady-state erosion rates at normal incidence for a series of $Al_2O_3$-SiC(w) composites using 143 μm diameter SiC erodents. The weight percent of whiskers of each composite is: open circles–0%, open squares–5%, open triangles–15%, and solid circles–25%.

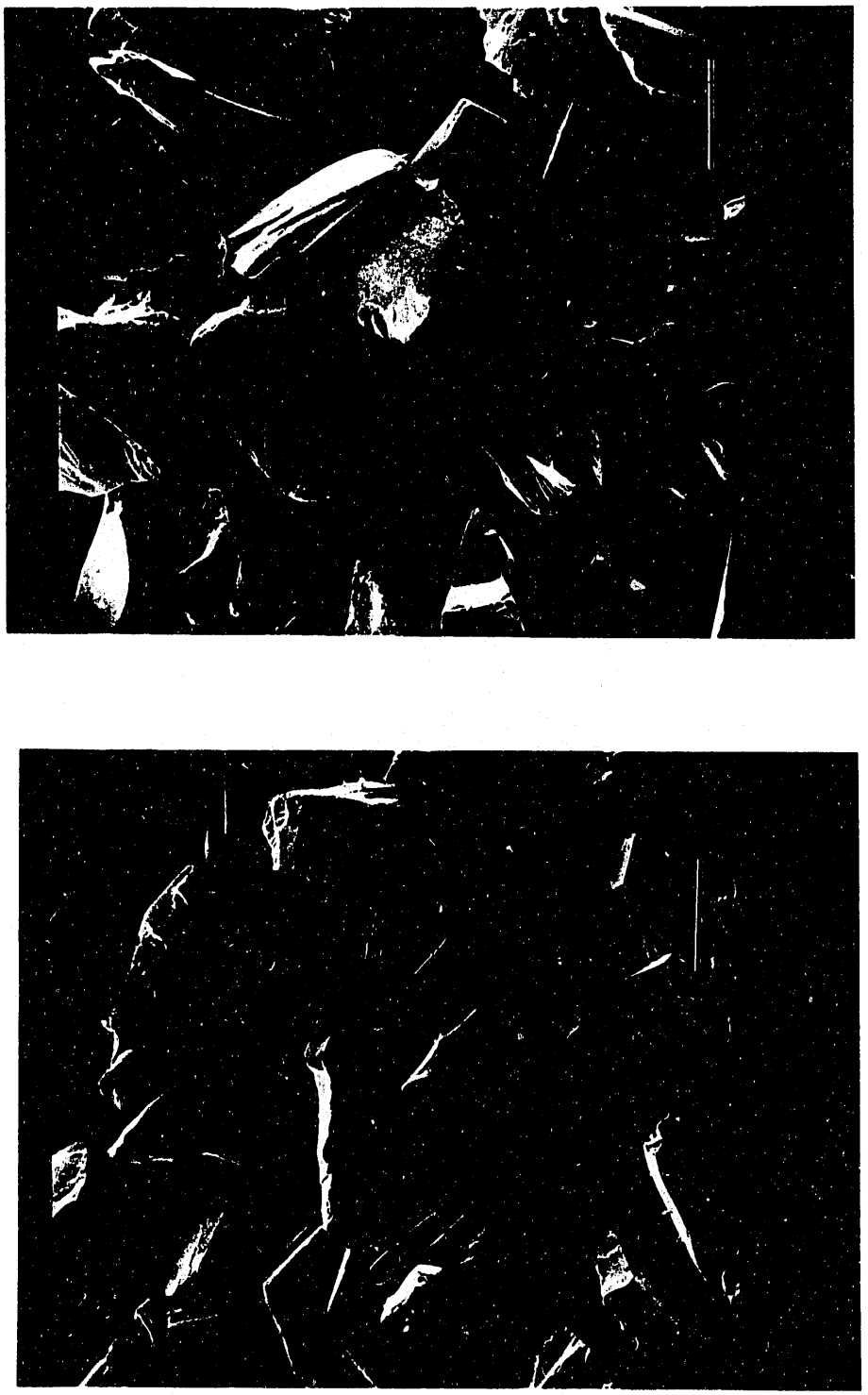

Figure 3. Scanning electron microscopy of 143 μm diameter SiC erodent: 3A–as received and 3B–after impacting a $Si_3N_4$ specimen at 100 m/s at normal incidence. The marker is 100 μm.

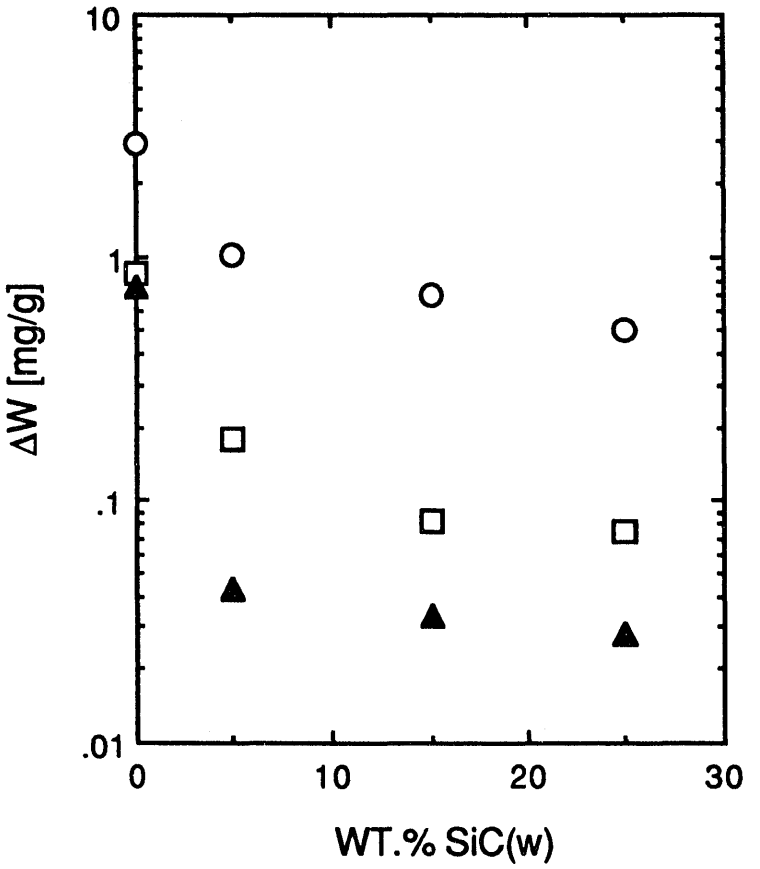


Figure 4. Steady-state erosion rate measured at normal incidence for an impacting velocity of 100 m/s using 143 μm diameter erodents of SiC (circles), $Al_2O_3$ (squares) and a 75% $Al_2O_3$ - 25% $ZrO_2$ abrasive (triangles).

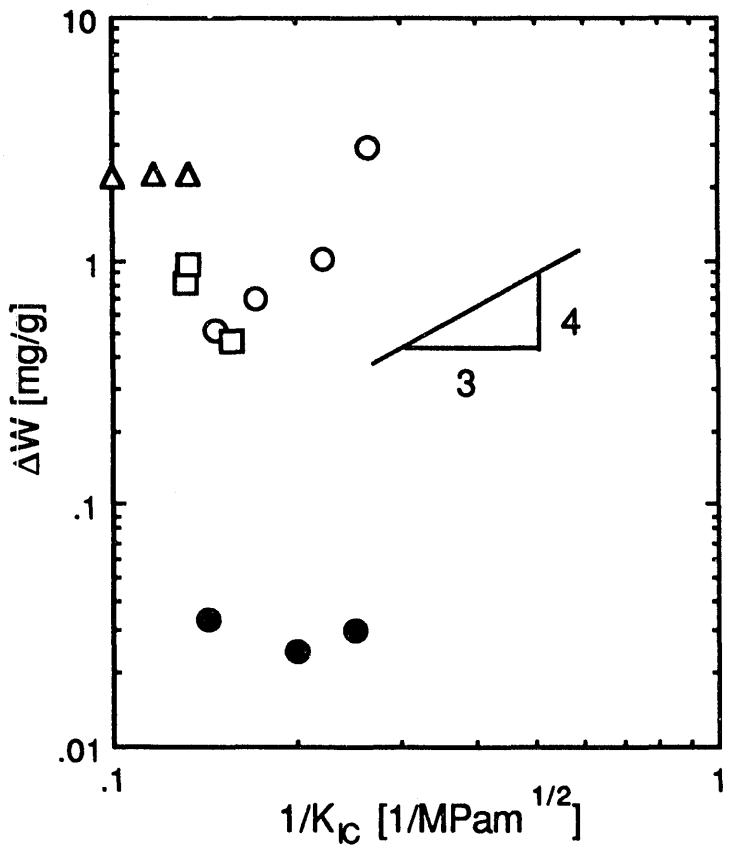


Figure 5. Steady-state erosion rate versus $1/K_{IC}$ for four whisker-reinforced composites measured using 143 μm diameter SiC abrasives. Symbols are $Si_3N_4$ (squares), $Al_2O_3$-SiC(w) (open circles), $Si_3N_4$-SiC(w) (filled circles) and $Y_2O_3$-stabilized $ZrO_2$-$Al_2O_3$(w) (triangles).

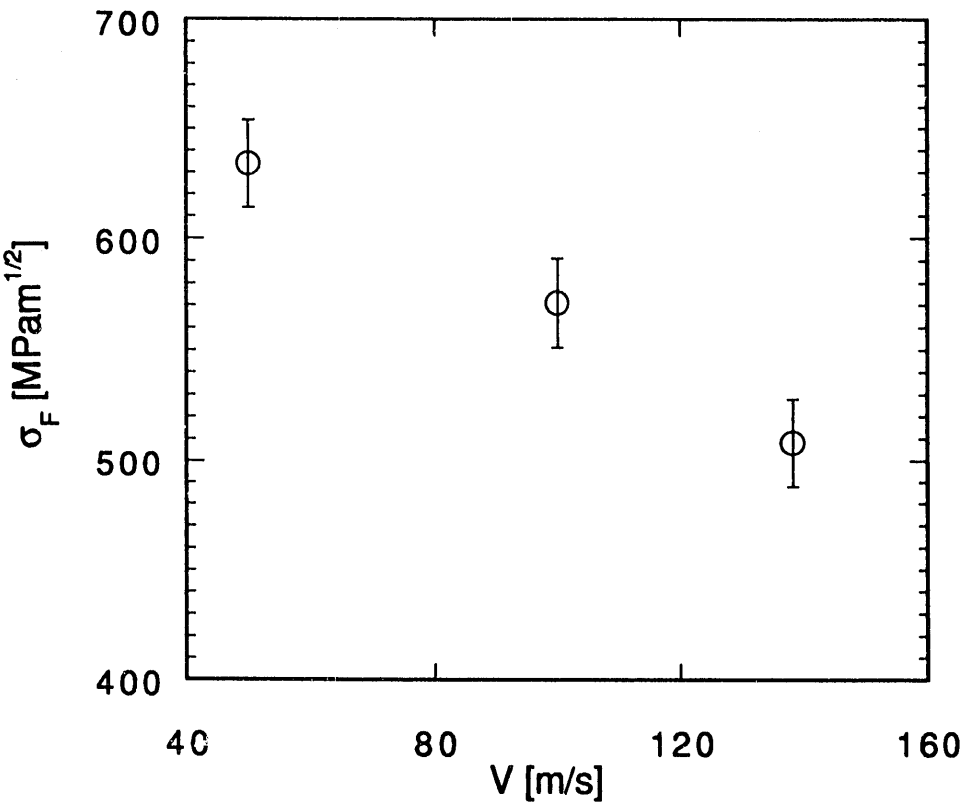


Figure 6. Fracture stress of an "*in-situ*" reinforced $Si_3N_4$ versus 143 μm mean diameter $Al_2O_3$ particle impact velocity under steady-state erosion conditions.

# END

DATE
FILMED
2/9/93